Applied Catalysis B: Environmental 257 (2019) 117943

Contents lists available at ScienceDirect

Applied Catalysis B: Environmental

journal homepage: www.elsevier.com/locate/apcatb

Pt/Al_2O_3 with ultralow Pt-loading catalyze toluene oxidation: Promotional synergistic effect of Pt nanoparticles and Al_2O_3 support

Tao Gan[a], Xuefeng Chu[b], Hui Qi[c], Wenxiang Zhang[a,*], Yongcun Zou[a], Wenfu Yan[a], Gang Liu[a,*]

[a] State Key Laboratory of Inorganic Synthesis and Preparative Chemistry, College of Chemistry, Jilin University, Changchun, 130012, China
[b] Jilin Provincial Key Laboratory of Architectural Electricity & Comprehensive Energy Saving, School of Electrical and Electronic Information Engineering, Jilin Jianzhu University, Changchun 130118, China
[c] The Second Hospital of Jilin University, Changchun 130041, China

ARTICLE INFO

Keywords:
Catalytic oxidation of toluene
Supported-Pt catalysts
Al_2O_3 support
Molecular O_2 activation
Synergistic effect

ABSTRACT

A kind of highly efficient and low cost supported-Pt catalyst for oxidation of toluene is obtained through controlling both the chemical state of Pt active sites and surface properties of supports. The optimized Pt/Al_2O_3 catalyst with Pt loading as low as 0.1 wt% could completely convert toluene (1000 ppm) to CO_2 at about 180 °C under a space velocity of 24,000 mL g^{-1} h^{-1}. It also exhibits a high stability and moisture resistance properties under reaction atmosphere. TOF value calculated with the dispersion of Pt can reach 0.0685 s^{-1}, representing a high utilization efficiency of Pt. A series of characterizations are carried out to investigate the key factors affecting the catalytic performance of Pt/Al_2O_3, and disclose the concrete role of Pt and Al_2O_3 in the activation of molecular oxygen and toluene. *In situ* DRIFTS and EPR results show that Pt is the active center for O_2 activation. Metallic Pt nanoparticles (Pt^0) can activate the molecular O_2 even at room temperature. Al_2O_3 offers sites for the adsorption of toluene and desorption of CO_2 product. The weak and medium strength of acid-base sites favorite the adsorption and desorption process. The oxidation of toluene over Pt/Al_2O_3 obeys modified L-H mechanism. The synergistic effect of metallic Pt nanoparticles and suitable Al_2O_3 support is critical for obtaining highly efficient Pt-based catalysts with low Pt contents for toluene oxidation.

1. Introduction

Toluene is widely used as solvents in the industrial processes of paints, adhesives, rubbers and leathers et al., and also used as additives for a high-octane gasoline. As one of typical volatile organic compounds (VOCs) pollutants, gaseous state toluene is not only harmful to human health, but also causes environment problems such as photochemical smog and ozone pollution. Catalytic oxidation of toluene has been recognized as an effective process for toluene elimination due to its lower energy consumption and the absence of secondary pollution [1–3]. Air is the sole and green source of oxygen in this process, and the products are only carbon dioxide and water. But this method still faces a series of challenges in the practical application. One is that the catalyst needs to achieve complete conversion of toluene at the lowest possible reaction temperature due to the requirement of energy saving. Energy consumption is generally the first problem that would be considered in the process of industrial implementation, especially for the exhaust gas treatment [4]. In addition, the cost of the catalyst and the tolerance of the catalyst to the moisture of the reaction atmosphere are also important for the practical application.

Up to now, a great number of catalysts have been reported that are active for the oxidation of toluene. However, considering the reaction temperature, supported noble-metal catalysts (especially Pt-based catalysts) still are the most excellent ones for this reaction. Many supported Pt catalysts can achieve complete conversion of toluene at a temperature below 200 °C. The bottleneck for these catalysts is the cost problem because such high activities are nearly all achieved under high Pt loading (no less than 0.5 wt%) [5–10]. The price and scarcity limit of Pt element determine the high cost of catalyst with large amount of Pt. Moreover, some reports showed that the water vapor in the reaction atmosphere could lower the activity of supported-Pt catalysts [11]. It would also affect the large-scale application of Pt-based catalysts since the water vapor is inevitable in most of industrial exhaust. Therefore, it is still desirable to develop highly efficient supported-Pt catalysts with both low cost and water resistance capability.

Reducing the loading amount of Pt is undoubtedly an effective means to solve the cost problem. But it is not easy to be realized since it usually causes a significant decrease of catalytic activity with the

* Corresponding authors.
E-mail addresses: zhwenx@jlu.edu.cn (W. Zhang), lgang@jlu.edu.cn (G. Liu).

https://doi.org/10.1016/j.apcatb.2019.117943
Received 29 December 2018; Received in revised form 3 May 2019; Accepted 6 July 2019
Available online 08 July 2019
0926-3373/

decline of Pt contents [12,13]. For achieving above aim, it can be thought primarily to carefully design the Pt sites [5,14,15]. And another one should be the construction of the catalyst supports [16]. The supports certainly not just act as a role of dispersing metal active sites when the amount of Pt decreases to a quite low level. A significant synergistic effect between Pt sites and catalyst supports must be present in the promising catalysts. But all these designs should base on the clear mechanism of toluene oxidation. Although the reaction mechanism has been mentioned in some reports, the concrete roles of Pt and supports in the activation of molecular oxygen and toluene are still uncertainty until now [6,16–19]. It has become the major obstacle to successfully develop highly efficient supported catalysts with low Pt contents.

Hence, we carry out this work through controlling both the chemical state of Pt active sites and surface properties of supports. The aims are not only to obtain highly efficient and low-cost Pt-based catalysts but also to clarify the reaction mechanism, especially the roles of Pt and supports in the activation of molecular oxygen and toluene. Alumina is chosen as a catalyst support because of its low cost, ready availability and low toxicity. A kind of Pt/Al_2O_3 catalyst with ultralow Pt loading (0.1 wt%) is screened, which could completely convert toluene (1000 ppm) to CO_2 at about 180 ℃. TOF value calculated with the dispersion of Pt can reach 0.0685 s^{-1}, which represents a high utilization of Pt. Interestingly, it also exhibits a high stability and a moisture resistance property in the reaction process. A series of characterizations, including *in situ* DRIFTS and EPR, are carried out to investigate the physic-chemical properties of the catalysts and clarify their roles in the activation of toluene and molecular O_2. This work may shed light on the design of efficient Pt-based catalysts for toluene oxidation with low Pt contents.

2. Experimental section

2.1. Materials

H_2PtCl_6•$6H_2O$ was purchased from Sinopharm Chemical Reagent Co., Ltd. Ammomia solution, NaOH and Ethylene glycol were obtained from Beijing Chemical Works. $Al(NO_3)_3$•$9H_2O$ and Na_2CO_3 was purchased from Tianjin Fuchen chemical reagents factory. All chemical reagents were analytical grade and without purification before used.

2.2. Catalyst preparation

The Al_2O_3 support was obtained by a precipitation method with NH_3•H_2O (12 wt%) or Na_2CO_3 (1 M) as precipitant, respectively. Typically, 40 g $Al(NO_3)_3$•$9H_2O$ was dissolved in 200 mL distilled water. The pH value was adjusted to 5 using the precipitant. The mixture was stirred for 2 h and then was dried out at 80 ℃. The obtained solid was calcined in muffle furnace at 600 ℃ for 3 h. The product prepared with NH_3•H_2O was denoted as Al_2O_3(A). The product prepared with Na_2CO_3 was washed with distilled water and filtered to remove excessive Na ions, and then dried at 100 ℃ for 5 h. The resultant solid was denoted as Al_2O_3(S).

The Pt/Al_2O_3 catalysts were prepared by a colloid deposition method and a traditional impregnation method, respectively. The content of Pt of all catalysts was controlled at about 0.1 wt% determined by inductively coupled plasma atomic emission spectrometer (ICP). As for the colloid deposition method, Pt colloids were prepared in advance as described in our earlier works [20,21]. Al_2O_3 was added to the Pt colloid under the vigorous stirring for 2 h. The mixture was heated at 80 ℃ for 10 h. The final product was filtered and washed thoroughly with distilled water until no chloride ions could be detected. Then the solid was dried at 100 ℃ for 3 h. All catalysts were calcined at 200 ℃ for 2 h in a flow of 20 vol% O_2/Ar. According to the difference of Al_2O_3 support, the resultant catalysts were denoted as Pt/Al_2O_3(A) and Pt/Al_2O_3(S), respectively. The sample of Pt/Al_2O_3(S) calcined at 600 ℃ was denoted as Pt/Al_2O_3(S)-T.

As for the traditional impregnation method, the Al_2O_3(S) was chosen as a support and added into the H_2PtCl_6 solution. After a brief mixing at room temperature, the solution was evaporated to dryness under the stirring at 80 ℃. The obtained solid was calcined in muffle furnace at 400 ℃ for 2 h, and then washed by distilled water until no chloride ions could be detected. After complete drying at 100 ℃ for 3 h, the catalyst was calcined at 200 ℃ for 2 h in a flow of 20 vol% O_2/Ar. The resultant catalyst was denoted as Pt/Al_2O_3(S)-I. Pt/Al_2O_3(S)-IR was prepared by reducing the Pt/Al_2O_3(S)-I in a flow of 5 vol% H_2/Ar at 400 ℃ for 2 h.

2.3. Catalyst characterization

Powder X-ray diffraction (XRD) patterns are recorded on a Rigaku X-ray diffractometer using Cu Kα radiation (50 kV, 200 mA). The scanning rate is 10°/min from 10° to 70°. N_2 adsorption/desorption isotherms at 77 K are measured using a Micromeritics ASAP 2010 N analyzer. The surface areas are calculated using the Brunauer–Emmett–Teller (BET) method. The pore size distributions are estimated using the Barrett-Joyner-Halenda (BJH) method. High-resolution transmission electron microscopy (HRTEM) observations are carried out on a JEOL JEM-2100 F instrument equipped with an energy dispersive X-ray (EDX) spectroscope, the operating voltage is 200 kV. X-ray photoelectron spectroscopy (XPS) is recorded on a Thermo ESCA LAB 250 instrument with an Al Kα source (1486.6 eV).

Temperature programmed desorption (TPD) is recorded on a ChemBET Pulsar TPR/TPD instrument. The spectrum is obtained by subtracting the blank spectrum of the sample. NH_3 and CO_2 are used as probe molecules to detect the acidic and basic properties of sample, respectively. Typically, 50 mg of catalysts are pretreated at 300 ℃ in N_2 flow for 30 min, and then cooled to 50 ℃ for probe molecule adsorption. 30 min later, stopping the adsorption process and sweeping the samples at 100 ℃ in He flow for 1 h. The samples are heated to 600 ℃ in He flow accompany with the data recording, and the heating rate is 10 ℃/min. As for C_7H_8-TPD, 50 mg of catalysts are pretreated at 300 ℃ in N_2 flow for 30 min and cooled to 50 ℃ for toluene adsorption. Treating the samples at 120 ℃ in He flow for 1 h and record the signal with the increase of temperature. Toluene is introduced by a bubble apparatus. The blank spectrum of the sample is measured under the same conditions except for the adsorption procedure.

In situ DRIFTS is performed on a Nicolet 6700 spectrometer. The procedure of CO adsorption is as follows: the catalysts are pretreated at 200 ℃ for 5 min in N_2 flow. After cooling to room temperature, the spectrum is collected and used as background. Subsequently, it is changed to the CO/Ar gas for adsorption and switched back to N_2 for removing the gas phase CO. The spectra are recorded at steady state. As for toluene adsorption, the steps are as follows: the samples are firstly pretreated at 300 ℃ for 5 min in N_2 flow, and then cooled to room temperature; the spectrum is recorded and used as the background; toluene is introduced successively by gas bubbling method with N_2 as a carrier gas; the spectra are collected under steady state at different temperatures. As for the investigation of toluene oxidation, the same pretreatment is carried out and the spectrum of background is recorded at 140 ℃. Toluene is introduced in the sample cell by carrier gas. The spectra are collected under steady state by step increase the temperatures. The switch of N_2 and 20 vol% O_2/Ar is carried out to create the specific atmosphere. EPR spectra are recorded on a JES-FA 200 EPR spectrometer. Samples with 0.5% Pt loading are used. All samples are pretreated with 300 ℃ in 20 vol% O_2/Ar for 0.5 h before testing.

2.4. Catalytic performance tests

Catalyst evaluation is carried out in a continuous-flow fixed-bed reactor. 100 mg of the catalyst, sieved to a particle size of 40–60 mesh, is placed in a central position of quartz flow microreactor on a quartz wool plug. The air stream which passes through the saturators (kept in

an ice bath) is mixed with another air stream to achieve the toluene vapor concentration of 1000 ppm in the experiment. The total flow rate of feed stream is 40 mL·min^{-1}, giving a space velocity (SV) at 24,000 mL·g^{-1} h^{-1}. Temperature is measured in the middle of the catalyst bed by means of a K-type thermocouple. The gas lines are heated at 120 ℃, aiming to minimize the adsorption of toluene on the tube walls. The analysis system consists of a gas chromatograph (INESA, GC-122) equipped with a FID detector for toluene, and a TCD detector for CO_2. Water is introduced into the reaction system by a temperature-controlled bubble apparatus.

For calculating apparent activation energy, reaction rate for toluene oxidation at different temperatures are evaluated by reducing the mass of catalysts to 50 mg to ensure the conversion of toluene is lower than 15%. The reaction rate is calculated as follows:

$$r_{tol} = \frac{X_{tol} F_{tol}}{m_{cat}}$$

where X_{tol} is the toluene conversion at different temperatures, F_{tol} is the molar flow rate of toluene and m_{cat} is the mass of catalyst.

The activation energies are calculated using the Arrhenius relationship as follows:

$$\ln k = -\frac{E_a}{RT} + lnA$$

where E_a is the apparent activation energy and A is the pre-exponential factor.

For calculating turnover frequency (TOF), the total gas flow rate is 80 mL·min^{-1} and the mass of catalyst is 20 mg to achieve the SV = 240000 mL·g^{-1} h^{-1}. The TOF is obtained by controlling the reaction temperature to make sure the conversion of toluene is lower than 15%. The result is tested by three times for the average value. The TOF is calculated based on the reaction rate as follows:

$$\text{TOF} = \frac{r_{tol} M_{Pt}}{X_{Pt} D_{Pt}}$$

Where M_{Pt} is the molar weight of Pt and X_{Pt} is the percentage of Pt on catalyst. D_{Pt} is the dispersion of 0.1% Pt, which is estimated by the equation:

$$D_{Pt}/\% = \frac{600 M_{Pt}}{\rho N_A A_{Pt} d_{Pt}}$$

where the M_{Pt} is 195.084 g·mol^{-1}, ρ is the density of Pt (21.45 g·cm^{-3}), N_A is the Avogadro constant as 6.02×10^{23} mol^{-1}, A_{Pt} is the cross section area of Pt atom (8.06×10^{-20} m^2·atom^{-1}), d_{Pt} means the average size of Pt nanoparticles which is estimated by the TEM images, d_{Pt} = 3.35 nm (Fig. S1).

3. Results and discussions

3.1. Catalytic performance of Pt/Al_2O_3 with ultralow Pt loading

The catalysts are screened *via* investigating the dependence of catalytic activity on the surface properties (especially surface acid-base properties) of Al_2O_3 support and the chemical state of Pt nanoparticles. Two kinds of Al_2O_3 supports prepared with different precipitants are adopted, which generally possess different surface acid-base properties. For tuning the chemical state of Pt nanoparticles, a colloid deposit method and a traditional impregnation method are carried out, respectively. The former method has been demonstrated in our previous work to be an effective method to form metallic Pt nanoparticles with uniform particle size [20,21], and the later one usually leads to a relatively strong interaction between Pt nanoparticles and oxide supports [22]. In addition, post thermal and reduction treatments are also carried out for further tuning the chemical states of Pt nanoparticles on the surface of catalysts.

Fig. 1 shows the catalytic toluene oxidation performance of different

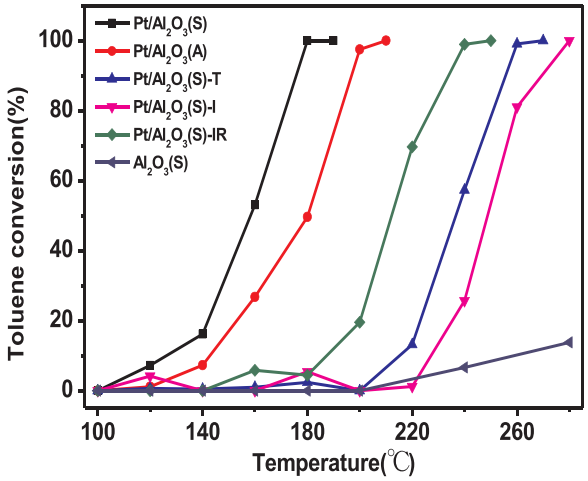

Fig. 1. Toluene conversion as a function of temperature over different samples.

Pt/Al_2O_3 catalysts and pure Al_2O_3. Without the use of catalysts, no toluene conversion is observed during the entire temperature region (not shown here). Over pure Al_2O_3, only very low conversion (less than 7%) of toluene can be observed when reaction temperature is up to 240 ℃.As for Pt/Al_2O_3, the toluene catalytic conversions over these catalysts exhibit S-shaped curves. The toluene conversion increases upon the increase of reaction temperature. It should be noted that the loading amounts of Pt in all Pt/Al_2O_3 catalysts are controlled at 0.1 wt%. It is confirmed that nearly all toluene is selectively converted to CO_2 over Pt/Al_2O_3 catalysts, so we mainly analyze the dependence of the toluene conversion on reaction temperature in the following work. With Pt colloids as a precursor, Pt/Al_2O_3(S) exhibits obviously higher activity than that of Pt/Al_2O_3(A) (see in Fig. 1). T_{50} (the reaction temperature of toluene with 50% conversion) and T_{100} (complete conversion temperature of toluene) are achieved at 157 ℃, 180 ℃ for Pt/Al_2O_3(S) and 180 ℃, 210 ℃ for Pt/Al_2O_3(A). This result means that Al_2O_3(S) is more suitable than Al_2O_3(A) to serve as a support for Pt-based catalyst in catalytic toluene oxidation. It should be noted that trace amount of sodium present in above catalysts. For completely excluding the influence of sodium on the catalytic results, the catalysts loaded with different amount sodium ions are investigated (see in supporting information, Fig. S2A and Fig. S2B). Little positive effect can be observed in the presence of sodium ions. On the contrary, the activity decreases significantly when the sodium contents increase to 5.0 wt%.

With Al_2O_3(S) as a support, catalytic activity of Pt obtained with different method or post-treatment is investigated (Fig. 1). Pt/Al_2O_3(S) prepared with a colloid deposit method exhibited significantly high activity than that of Pt/Al_2O_3(S)-I prepared with an impregnation method. According to our previous work, Pt nanoparticles obtained with colloid deposition method are mainly present as metallic state (Pt^0) [20,21], while impregnation method usually form Pt species with positive valence [23]. Combined with catalytic results, it indicates that metallic Pt should be more suitable for the oxidation of toluene.

To test this hypothesis, further thermal and reduction treatment are separately carried out over Pt/Al_2O_3(S) and Pt/Al_2O_3(S)-I catalysts. It is known that thermal treatment could increase the interaction between Pt and the support [24,25], and the reduction treatment usually leads to more metallic Pt species [26]. The resultant Pt/Al_2O_3(S)-T exhibits a much lower activity than that of Pt/Al_2O_3(S), while Pt/Al_2O_3(S)-IR shows a higher activity compared with Pt/Al_2O_3(S)-I. In addition, the apparent activation energies are calculated by using the Arrhenius relationship (Fig. 2). The activation energy over Pt/Al_2O_3(S) is 65.9 kJ·mol^{-1}, which is followed by Pt/Al_2O_3(A) (91.0 kJ·mol^{-1}) and Pt/Al_2O_3(S)-I (154.0 kJ·mol^{-1}). All these results preliminarily confirm the hypothesis that metallic Pt is suitable for catalytic toluene oxidation, and the properties of Al_2O_3 support have significant influence on

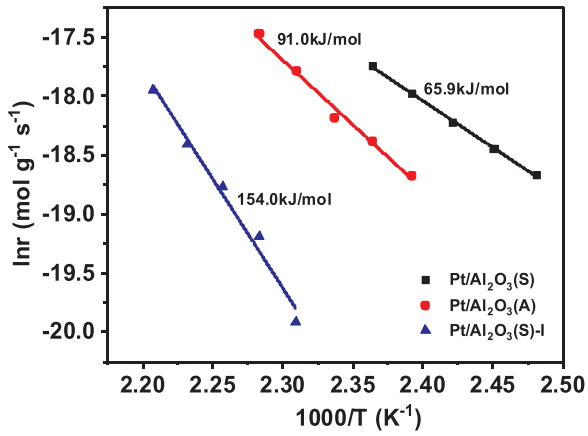

Fig. 2. Arrhenius plots for the toluene oxidation over different Pt/Al_2O_3 catalysts.

the activity. More details will be discussed below.

Compared with the excellent catalysts reported in literatures, Pt/Al_2O_3(S) catalyst exhibits a higher or at least comparable low-temperature activity under the similar reaction conditions (see Fig. S3 and Table S1) [7,9,10,19,27–31]. It should be emphasized that such high activity at low temperature in our case is obtained upon the loading amount of Pt as low as 0.1 wt%, which is much lower than that of current works. The turnover frequency (TOF) for toluene oxidation is evaluated with a low conversion (less than 15%) of toluene under the space velocity (SV) of 240000 $mL{\cdot}g^{-1}\,h^{-1}$ and reaction temperature of 160 ℃ (details shown in the experimental section). The value of TOF over Pt/Al_2O_3(S) catalyst is 0.0685 s^{-1}, which is calculated with the dispersion of Pt loading on the support. If counted with the amount of Pt, the conversion number of toluene over Pt/Al_2O_3(S) catalyst is 0.023 $mol_{toluene}{\cdot}mol_{Pt}^{-1}{\cdot}s^{-1}$. All these values are higher than most of the literature results, showing a high utilization of Pt element in Pt/Al_2O_3(S) catalyst. We also investigate the activity of supported Pt catalysts with different metal oxides as supports (Fig. S4). Only Pt/ZnO possesses comparable initial activity with Pt/Al_2O_3(S), but deactivation can be observed when extending the detection time. Moreover, it is known that Al_2O_3 is a low-cost oxide support. In our case, it need not any other transition metal or metal oxides as catalyst promoters. All these results indicate that Pt/Al_2O_3(S) catalyst possesses good potential for application.

Pt/Al_2O_3(S) also exhibits a high stability in the reaction process. The test at the reaction temperature of 180 ℃ showed that Pt/Al_2O_3(S) has maintained a high and stable toluene conversion rate (Fig. 3A). Only a small fluctuation can be observed during the long time investigation and this fluctuation can be eliminated when the reaction temperature increase to 185 ℃. In addition, Pt/Al_2O_3(S) exhibits a desirable water resistance property during the reaction process. It is known that water vapor always exists in exhaust emission. Many researches show that the water caused a decrease in activities over a series of catalysts, and it is regarded as a typical poison in the catalytic oxidation of VOCs [11,32,33]. In our case, when 4.5 vol% water vapor is introduced into the reactor, there is almost no change can be observed in toluene conversion curve (Fig. 3B). This result shows that water vapor in the reaction atmosphere has little influence on the activity of Pt/Al_2O_3(S).

3.2. Characterizations of Pt/Al_2O_3 catalysts

A series of characterizations are carried out over typical Pt/Al_2O_3 catalysts to investigate the key factors that affecting the catalytic performance of Pt/Al_2O_3 with such low Pt loading amount. Fig. 4 shows the XRD patterns of Pt/Al_2O_3(S), Pt/Al_2O_3(A) and Pt/Al_2O_3(S)-I. All the diffraction peaks could be ascribed to the phase structure of Al_2O_3 support, including γ-phase Al_2O_3 and Bayerite [34,35]. It is known that

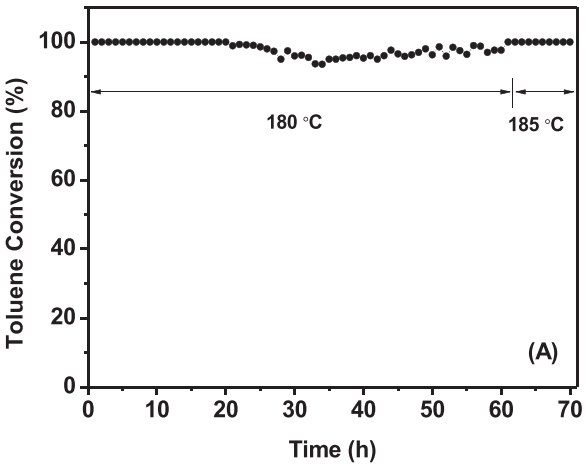

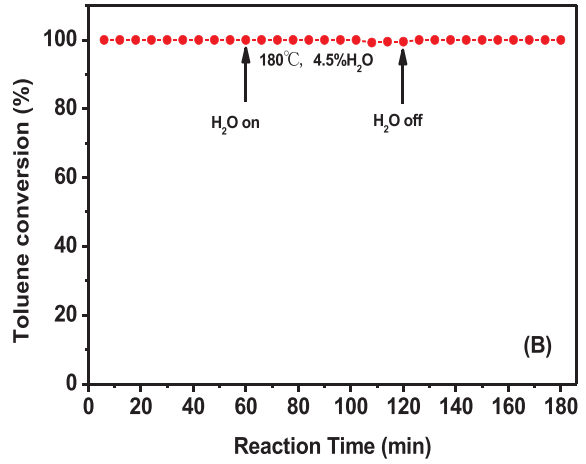

Fig. 3. (A) Stability test of Pt/Al_2O_3(S) catalyst for toluene conversion. (B) Water effect on toluene conversion over Pt/Al_2O_3(S) catalyst. Gas composition: 1000 ppm toluene, air balance, and SV = 24,000 $mL{\cdot}g^{-1}\,h^{-1}$.

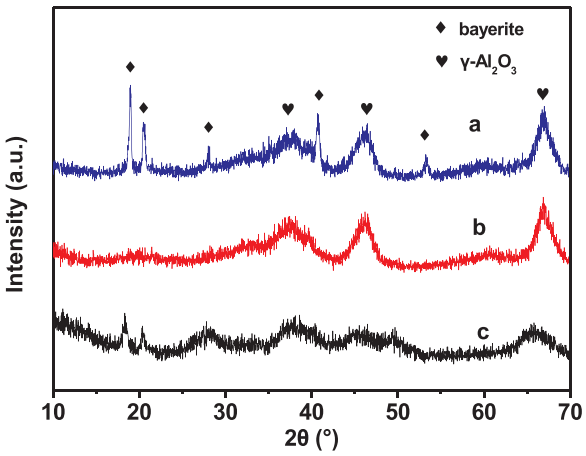

Fig. 4. XRD patterns of typical Pt/Al_2O_3 catalysts: (a) Pt/Al_2O_3(S), (b) Pt/Al_2O_3(S)-I, (c) Pt/Al_2O_3(A).

the colloid solution exhibits strongly alkaline property, while $H_2PtCl_6{\bullet}6H_2O$ aqueous solution shows acid property. Considering the different preparation methods, the phase structure of these Pt/Al_2O_3

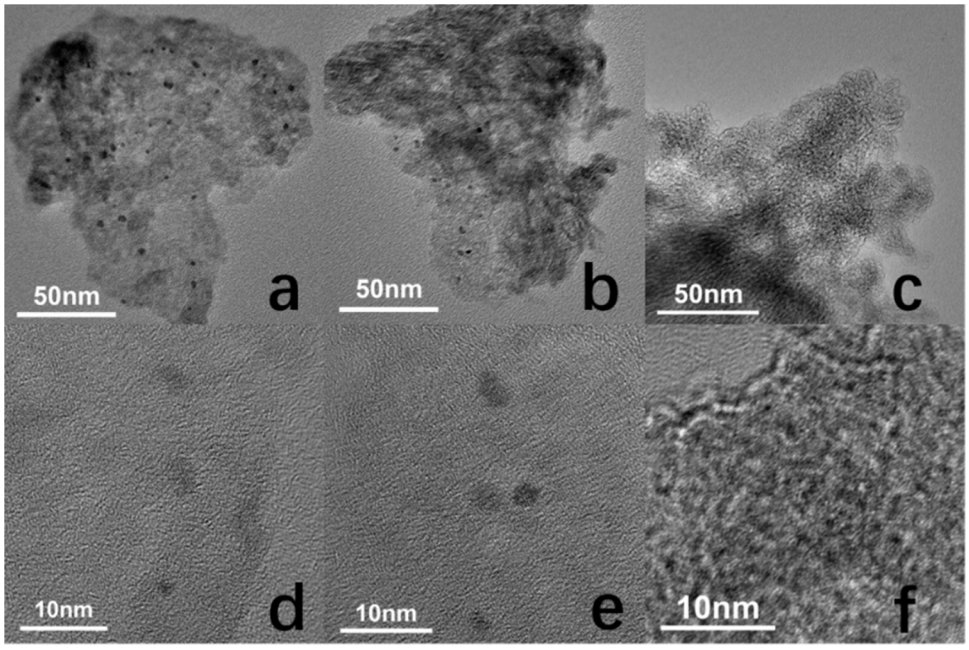

Fig. 5. TEM images of different Pt/Al_2O_3 catalysts: (a)(d) Pt/Al_2O_3(S), (b)(e) Pt/Al_2O_3(A), and (c)(f) Pt/Al_2O_3(S)-I.

catalysts are affected not only by the original properties of the Al_2O_3 supports, but also by the pH value of the solution in the loading process and the temperature of subsequent thermal treatment for obtaining Pt/Al_2O_3 catalysts. Alkaline condition is much easier to form Bayerite phase, while acid condition is more suitable for the formation of γ-phase Al_2O_3. Although certain amount of Bayerite is present in Al_2O_3(S) (Fig. S5), there is no direct correlation between this phase structure and catalytic toluene oxidation performance. This point is verified by a series of experiments (see in supporting information, Figs. S6 and S7). When thermal-treated Al_2O_3(S) is used as a support, the resultant catalyst without Bayerite phase exhibits similar activity to that of Pt/Al_2O_3(S) (Fig. S7).

In addition, no diffraction peaks assigned to Pt particles are observed in the three catalysts, which should be due to the low loading amount and highly dispersed states of Pt. This phenomenon is confirmed by the TEM images of these samples (Fig. 5). In the samples of Pt/Al_2O_3(S) and Pt/Al_2O_3(A), Pt is present as nanoparticles with 3–4 nm size, which is like the morphology of the as-synthesized Pt colloid (Fig. S8). As for Pt/Al_2O_3(S)-I, no particles can be observed in the detected region, and Pt should be present as very small entities, probably even atomically dispersed as ascertained by Kwak, Moses-DeBusk and Zhang et al. [22,36,37].

XPS is carried out to identify the chemical state of Pt in these Pt/Al_2O_3 catalysts (Fig. 6A). Due to the detection limit, Pt signals of 0.1 wt % Pt-content samples cannot be detected, so 0.5 wt% Pt/Al_2O_3 is used as a substitute for testing. Fig. 6A shows that Pt/Al_2O_3(A) and Pt/Al_2O_3(S) exhibit similar binding energy peak located at 313.5 eV, showing that Pt is mainly present as metallic state *i.e.* Pt^0 on the surface of Al_2O_3 supports. It means that Pt nanoparticles maintain the chemical states of their colloid precursors and are not affected by the surface properties of Al_2O_3 supports. As for Pt/Al_2O_3(S)-I, a peak centered at 315.8 eV can be observed, which indicates that positive charged Pt (including Pt^{2+} and Pt^{4+}) is present on the sample of Pt/Al_2O_3(S)-I. The dominant feature in this sample should be Pt-O. TEM result has shown that Pt on the sample of Pt/Al_2O_3(S)-I is present as very small entities. Although it cannot ensure these Pt species are present as single-atoms, the surface coordinatively unsaturated Al^{3+} centers are the most possible positions to stabilize these Pt species. According to the independent reports by Kwak and Yan [22,37], these Al^{3+} centers mainly come from pentacoordinate Al^{3+} species.

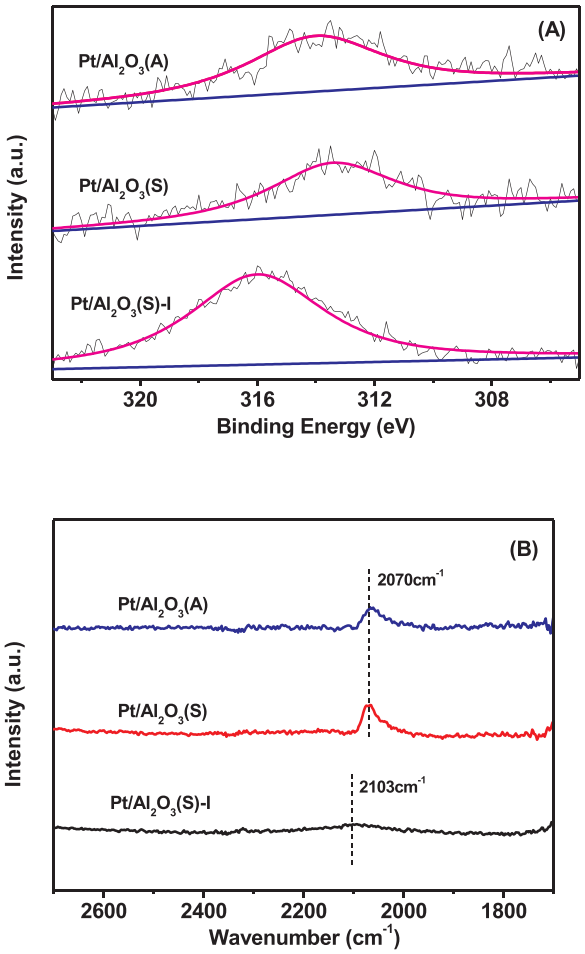

Fig. 6. (A) Pt $4d_{5/2}$ XPS spectra of different Pt/Al_2O_3 catalysts and (B) DRIFTS spectra of CO adsorption on different Pt/Al_2O_3 catalysts.

In-situ DRIFTS spectra of CO adsorption is further carried out to identify the chemical state of Pt on the sample of $Pt/Al_2O_3(S)$, $Pt/Al_2O_3(A)$ and $Pt/Al_2O_3(S)$-I. As shown in Fig. 6B, a signal at 2070 cm^{-1} can be observed in the spectra of $Pt/Al_2O_3(S)$, $Pt/Al_2O_3(A)$, which can be ascribed to CO adsorption on metallic state Pt nanoparticles [37,38]. As for $Pt/Al_2O_3(S)$-I, the signal shifts to 2103 cm^{-1}, which indicates that CO adsorbed on oxidize state Pt sites [39]. These results further confirm that Pt is mainly present as metallic state in $Pt/Al_2O_3(S)$ and $Pt/Al_2O_3(A)$, and oxidize state in $Pt/Al_2O_3(S)$-I. They are consistent with the results of XPS. The chemical states of Pt are mainly determined by the preparation method. Different Al_2O_3 supports have little effect on the properties of Pt nanoparticles.

3.3. Influence of Al_2O_3 support on catalytic toluene oxidation

Combined with the catalytic results and above characterizations, different catalytic activities of $Pt/Al_2O_3(S)$ and $Pt/Al_2O_3(A)$ in the toluene conversion should be ascribed to the different surface properties of Al_2O_3 support because they possess almost the same Pt active centers. Our experiment results could exclude the direct influence of phase structure of $Al_2O_3(S)$ and $Al_2O_3(A)$ on the catalytic activity of resultant catalysts (Fig S5). In addition, N_2-adsorption results show that $Pt/Al_2O_3(S)$ and $Pt/Al_2O_3(A)$ possess quite similar specific surface areas and porous properties (Table 1). Based on these results, we speculate that surface acid-base properties of different Al_2O_3 supports might be an important factor for catalytic performance, which would directly affect the adsorption or desorption of toluene over these catalysts.

NH_3-TPD and CO_2-TPD are carried out to detect the acid-base properties of $Pt/Al_2O_3(A)$ and $Pt/Al_2O_3(S)$ catalysts. NH_3-TPD shows that both $Pt/Al_2O_3(A)$ and $Pt/Al_2O_3(S)$ possess multiple acid sites, including weak, medium and relatively strong strength sites (Fig. 7A). Compared with the spectrum of $Pt/Al_2O_3(S)$, a relatively strong peak centered at about 376 ℃ can be observed on the spectrum of $Pt/Al_2O_3(A)$. It shows that the amount of strong acid sites over $Pt/Al_2O_3(A)$ is larger than that of $Pt/Al_2O_3(S)$. CO_2-TPD shows that $Pt/Al_2O_3(A)$ also possess larger amount of strong basic sites than $Pt/Al_2O_3(S)$ (Fig. 7B). While the amounts of weak and medium strength acid or base sites are similar over both $Pt/Al_2O_3(A)$ and $Pt/Al_2O_3(S)$ samples.

C_7H_8-TPD is carried out to detect the adsorption and desorption of toluene over $Pt/Al_2O_3(A)$ and $Pt/Al_2O_3(S)$. Fig. 7C shows that both samples are with excellent toluene adsorption capacity. But there are some obvious differences between $Pt/Al_2O_3(A)$ and $Pt/Al_2O_3(S)$. One is that the peak center of $Pt/Al_2O_3(A)$ locates at relatively high temperature region compared with that of $Pt/Al_2O_3(S)$. Another is that total desorption amount over $Pt/Al_2O_3(A)$, especially in the temperature region of 200–320 ℃, is obviously higher than that of $Pt/Al_2O_3(S)$. These differences show that the interaction between toluene and $Pt/Al_2O_3(A)$ is stronger than $Pt/Al_2O_3(S)$. This strong interaction should be correlated with the presence of strong acid-base sites on the surface of $Pt/Al_2O_3(A)$. This trend is also correlated well with the toluene conversion temperature over these two catalysts, which suggests that the adsorption of toluene over the supports has significantly effect on the catalytic activity.

In situ DRIFTS measurements are carried out to further detect the adsorption of toluene over Pt/Al_2O_3 and Al_2O_3 supports (Fig. 8A and B),

Table 1
N_2-adsorption results of different Pt/Al_2O_3 catalysts.

Sample	BET surface area ($m^2\,g^{-1}$)	Average pore width (nm)[a]	Pore volume ($cm^3\,g^{-1}$)[a]
$Pt/Al_2O_3(S)$	499	3.13	0.41
$Pt/Al_2O_3(A)$	495	3.10	0.40
$Pt/Al_2O_3(S)$-I	431	3.73	0.42

[a] The average pore width and pore volume are calculated with adsorption branch.

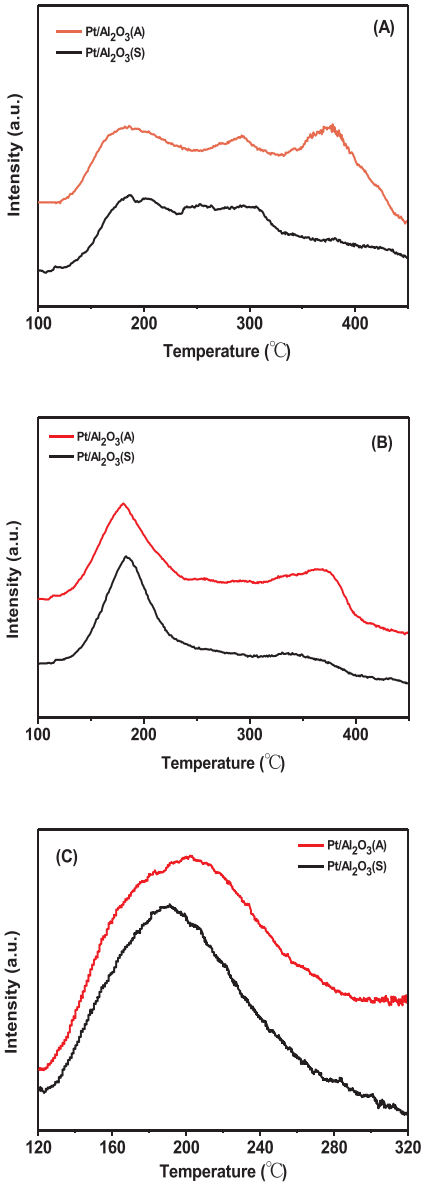

Fig. 7. (A) NH_3-TPD, (B) CO_2-TPD, and (C) C_7H_8-TPD over different Pt/Al_2O_3 catalysts.

in which the spectra of $Al_2O_3(S)$ and $Pt/Al_2O_3(S)$ are used as the background. It should be noted that there is no difference between the spectra of $Al_2O_3(S)$ and $Pt/Al_2O_3(S)$, which means that Pt has little influence on the adsorption of toluene. The bands at 3088, 3062 and 3030 cm^{-1} could be attributed to the C—H stretching vibrational bands of the aromatic ring [40–42]. The characteristic ν(C—H) bands at 2923 and 2880 cm^{-1} are assigned to the C—H asymmetric and symmetric stretching vibrations of the alkyl group [40–42], 1604 and 1496 cm^{-1} are belong to skeletal vibration of aromatic ring [40,41], 1380 and 1456 cm^{-1} are belong to the methyl group [40,41]. Interestingly, toluene adsorption correlated well with the consumption of surface hydroxyl groups over Al_2O_3. A negative peak can be observed at 3753 cm^{-1} and it accompanies with two new bands appeared at 3658 and 3693 cm^{-1}, suggesting that an interaction is present between toluene and hydroxyl groups. With the increase of temperatures, the intensities of these peaks are all become weak, indicating that desorption of toluene occurs when the temperature increases.

It is known that toluene is with weak basic property. DRIFTS spectra prove the interaction between toluene molecules and the surface hydroxyl groups of Al_2O_3. These hydroxyl groups are usually the acid sites

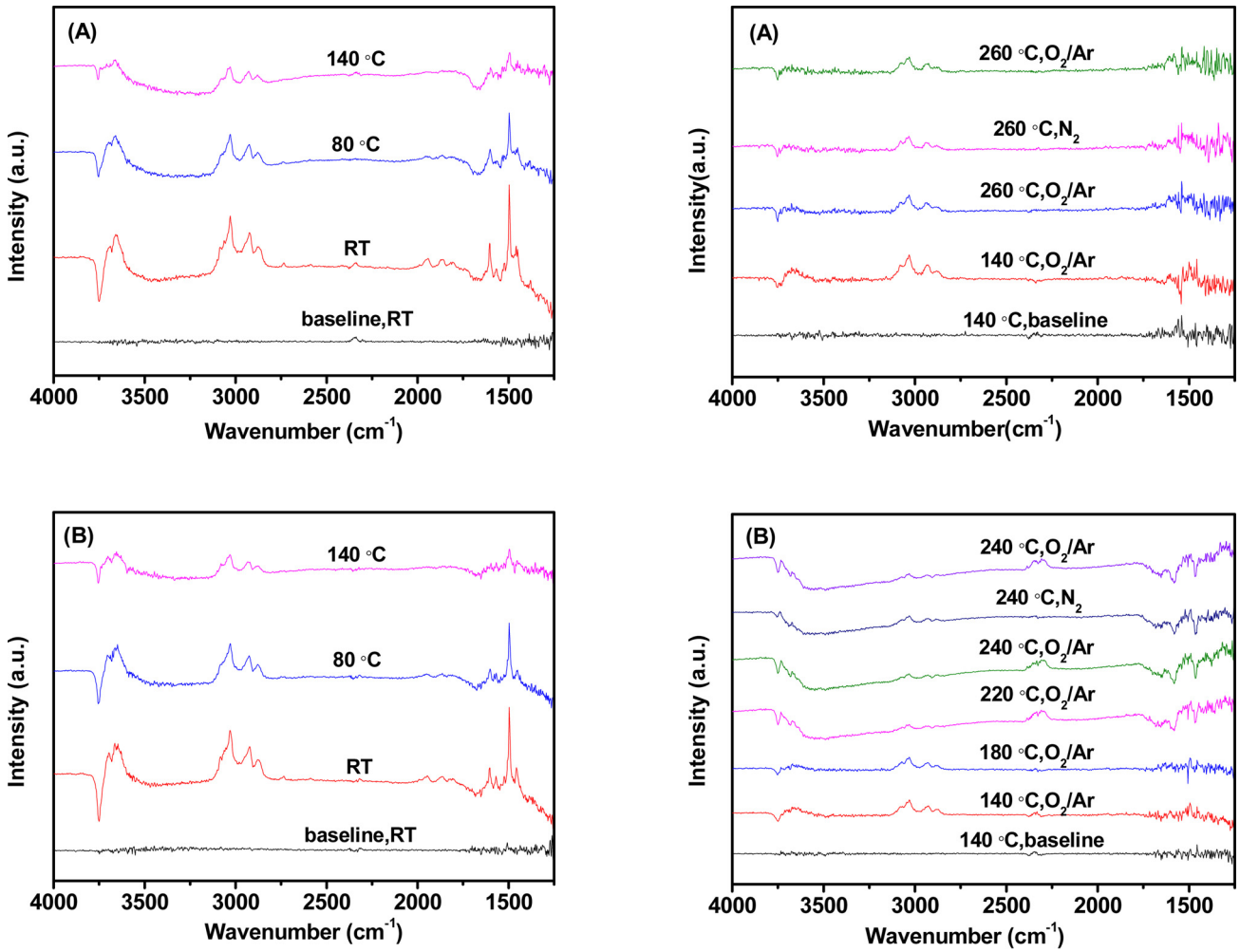

Fig. 8. DRIFTS spectra of toluene adsorption on (A) Al_2O_3(S) and (B) Pt/Al_2O_3(S).

of Al_2O_3. Combined with results of above three TPD spectra, the surface acidic sites of the support should directly contribute the adsorption of toluene. The strong acid sites on the surface of Pt/Al_2O_3(A) should cause the strong interaction between toluene and Pt/Al_2O_3(A). This strong interaction should be unfavorable for the conversion of toluene. With the same Pt nanoparticles as active sites, Pt/Al_2O_3(A) exhibits a lower activity than that of Pt/Al_2O_3(S). In addition, the strength of basic sites over the catalysts should also be correlated with the reaction results. Strong basic sites cause a strong interaction with CO_2 (the product of toluene oxidation) and decrease the desorption of them from the catalyst. It would hinder the reaction proceeding on the surface of catalysts at low temperatures. Therefore, it can be proposed that weak and medium strength of acid and base sites should facilitate this reaction due to the suitable adsorption and desorption behavior caused by these sites. It should be one of critical factors that Pt/Al_2O_3(S) exhibits excellent low-temperature activity for catalytic toluene oxidation.

3.4. Role of Pt nanoparticles on catalytic toluene oxidation

The oxidation of toluene over different samples is detected with *in situ* DRIFTS measurement. Different from the test of adsorption, N_2 and 20 vol% O_2/Ar separately act as the carrier gas to introduce toluene into the reaction cell. Fig. 9 shows the *in situ* DRIFTS spectra of Al_2O_3(S), Pt/Al_2O_3(S) and Pt/Al_2O_3(*S*)-I at different temperatures. We mainly focus on the bands in the range of 2880-3088 cm^{-1} and 2300-2350 cm^{-1}. The former one is ascribed to the vibrations of C—H from toluene molecules, and the later one can be ascribed to vibration of CO_2 formed in the reaction process [40–43]. As for pure Al_2O_3(S) support (Fig. 9A), nearly no change can be observed over the signals assigned to toluene, and no signals assigned to the CO_2 can be observed in the temperature range from 140 to 260 °C. It shows that the oxidation of toluene could not occur over pure Al_2O_3(S) support in this temperature range.

Fig. 9. *In situ* DRIFTS spectra of toluene oxidation over (A) Al_2O_3(S), (B) Pt/Al_2O_3(S), and (C) Pt/Al_2O_3(S)-I.

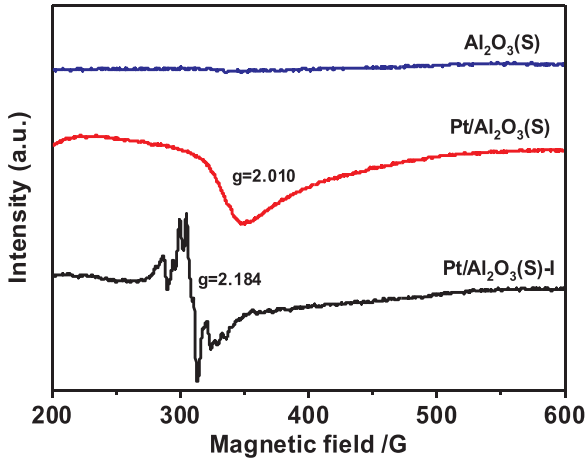

Fig. 10. EPR spectra of different samples at room temperature.

As shown in the spectra of $Pt/Al_2O_3(S)$, the conversion of toluene can be observed clearly when the temperature increased to 220 ℃, which accompany with an obvious signal assigned to the CO_2 (Fig. 9B). It can be confirmed that the oxidation of toluene to CO_2 occurs on the surface of $Pt/Al_2O_3(S)$ at this temperature. Compared with the results of $Al_2O_3(S)$, 0.1 wt% Pt nanoparticles in the $Pt/Al_2O_3(S)$ catalyst should be a critical factor. We have shown that the adsorption of toluene occurs on the surface of $Al_2O_3(S)$ support. The role of Pt nanoparticles in this reaction should be the sites for the activation of molecular O_2. We also carry out the DRIFTS investigation based on the switch between O_2/Ar and N_2 (Fig. 9B). It shows that the conversion of toluene depends significantly on the presence of O_2. The signals of CO_2 disappear immediately under the N_2 atmosphere. Compared with $Pt/Al_2O_3(S)$, the conversion of toluene to CO_2 over $Pt/Al_2O_3(S)$-I appears at much higher temperature (Fig. 9C). It means that the capability of Pt for O_2 activation in $Pt/Al_2O_3(S)$-I is much lower than that of $Pt/Al_2O_3(S)$.

The activation of molecular O_2 over these three samples is further detected by electron paramagnetic resonance (EPR, Fig. 10) at room temperature. When the samples are exposed to air, no apparent EPR signals are detected on pure $Al_2O_3(S)$ support. While an obvious signal with a *g* factor of 2.010 is observed on $Pt/Al_2O_3(S)$, which can be ascribed to surface superoxide radical anion $O_2^{\cdot-}$ species [44,45]. As for $Pt/Al_2O_3(S)$-I, this signal cannot be observed clearly. If it exists, the signal should be very weak and overlapped by the signals of paramagnetic platinum (Pt^{3+}) [46–48]. All these results confirm that O_2 can be easily activated by $Pt/Al_2O_3(S)$ even at room temperature.

For making sure the metallic Pt nanoparticles are the real active sites during the reaction, the used $Pt/Al_2O_3(S)$ catalyst is also characterized with XPS and *in-situ* CO-adsorption DRIFTS. For facilitating measurements, $Pt/Al_2O_3(S)$ with 0.5 wt% Pt is taken as a model. This catalyst is proved possessing excellent stability during the long time reaction test (Fig. S9). Both XPS and *in-situ* CO-adsorption DRIFTS results show that Pt is still present as metallic state after a long time reaction (Figs. S10 and S11A). Moreover, the catalyst after continuous reaction is further thermally treated in oxygen atmosphere (at 300℃ for 30 min in 20 vol% O_2/Ar flow). Surface Pt still maintains metallic state (Figs. S10 and S11B). It should be noted that this treating temperature is obviously higher than reaction temperature. All these results represent that metallic Pt nanoparticles is stable in the oxygen abundant reaction conditions. It could confirm that metallic Pt is the active center during the reaction.

According to above results, it is demonstrated that Pt nanoparticles play the role of active sites for molecular O_2 activation. Metallic state Pt is more favorable than the Pt with positive valence, which should be mainly due to the capacity of electron transfer from Pt to O_2. It is known that catalytic VOCs oxidation is determined by three main factors: the adsorption of VOCs molecules, the desorption of products (CO_2) and activation of molecular O_2. In our case, the excellent performance of $Pt/Al_2O_3(S)$ should be ascribed to both the active Pt for the molecular O_2 activation and suitable $Al_2O_3(S)$ for the adsorption-desorption process. The catalytic oxidation of toluene over $Pt/Al_2O_3(S)$ should obey the modified L-H mechanism (Scheme 1). The synergistic effect between Pt nanoparticles and $Al_2O_3(S)$ promotes the conversion of toluene over this catalyst with ultralow Pt contents.

4. Conclusion

Highly efficient Pt/Al_2O_3 catalyst with ultralow Pt contents has been prepared *via* controlling the chemical state of Pt and surface properties of Al_2O_3. The synergistic effect of metallic Pt nanoparticles and Al_2O_3 support with suitable acid-base sites is the key factor for the high activity of the catalyst for toluene oxidation. The oxidation of toluene over Pt/Al_2O_3 obeys modified L-H mechanism. Metallic Pt nanoparticles are the active centers for molecular O_2 activation, and Al_2O_3 offers sites for the adsorption of toluene and desorption of CO_2 product. The weak and medium strength of acid-base sites favorite the adsorption and desorption process. This work would shed light on the design of efficient and low-cost Pt-based catalysts for VOCs oxidation.

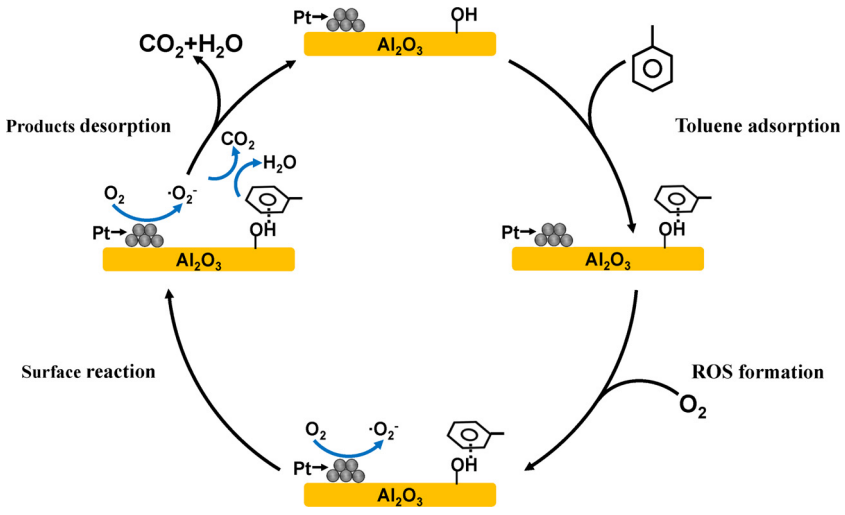

Scheme 1. Illustration of reaction process of toluene oxidation over Pt/Al_2O_3 catalyst. (ROS: reactive oxygen species).

Acknowledgements

The authors acknowledge support from the National Natural Science Foundation of China (21473073, 21473074), the Development Project of Science and Technology of Jilin Province (20170101171JC, 20180201068SF) and the Open Project of State Key Laboratory of Inorganic Synthesis and Preparative Chemistry (201703).

Appendix A. Supplementary data

Supplementary material related to this article can be found, in the online version, at doi:https://doi.org/10.1016/j.apcatb.2019.117943.

References

[1] M.S. Kamal, S.A. Razzak, M.M. Hossain, Catalytic oxidation of volatile organic compounds (VOCs) – a review, Atmos. Environ. 140 (2016) 117–134.
[2] L.F. Liotta, Catalytic oxidation of volatile organic compounds on supported noble metals, Appl. Catal. B: Environ. 100 (2010) 403–412.
[3] S. Scire, L.F. Liotta, Supported gold catalysts for the total oxidation of volatile organic compounds, Appl. Catal. B: Environ. 125 (2012) 222–246.
[4] J.J. Spivey, Complete catalytic oxidation of volatile organics, Ind. Eng. Chem. Res. 26 (1987) 2165–2180.
[5] K.J. Kim, H.G. Ahn, Complete oxidation of toluene over bimetallic Pt-Au catalysts supported on ZnO/Al_2O_3, Appl. Catal. B: Environ. 91 (2009) 308–318.
[6] V.P. Santos, S.A.C. Carabineiro, P.B. Tavares, M.F.R. Pereira, J.J.M. Orfao, J.L. Figueiredo, Oxidation of CO, ethanol and toluene over TiO_2 supported noble metal catalysts, Appl. Catal. B: Environ. 99 (2010) 198–205.
[7] C.Y. Chen, J. Zhu, F. Chen, X.J. Meng, X.M. Zheng, X.H. Gao, F.S. Xiao, Enhanced performance in catalytic combustion of toluene over mesoporous Beta zeolite-supported platinum catalyst, Appl. Catal. B: Environ. 140 (2013) 199–205.
[8] F. Rahmani, M. Haghighi, P. Estifaee, Synthesis and characterization of Pt/Al_2O_3–CeO_2nanocatalyst used for toluene abatement from waste gas streams at low temperature: conventional vs. plasma–ultrasound hybrid synthesis methods, Microporous Mesoporous Mater. 185 (2014) 213–223.
[9] Z. Abdelouahab-Reddam, R. El Mail, F. Coloma, A. Sepulveda-Escribano, Platinum supported on highly-dispersed ceria on activated carbon for the total oxidation of VOCs, Appl. Catal. A Gen. 494 (2015) 87–94.
[10] J.Y. Zhang, C. Rao, H.G. Peng, C. Peng, L. Zhang, X.L. Xu, W.M. Liu, Z. Wang, N. Zhang, X. Wang, Enhanced toluene combustion performance over Pt loaded hierarchical porous MOR zeolite, Chem. Eng. J. 334 (2018) 10–18.
[11] C.Y. Chen, Q.M. Wu, F. Chen, L. Zhang, S.X. Pan, C.Q. Bian, X.M. Zheng, X.J. Meng, F.S. Xiao, Aluminium-rich Beta zeolite-supported platinum nanoparticles for the low-temperature catalytic removal of toluene, J. Mater. Chem. A 3 (2015) 5556–5562.
[12] S.C. Kim, S.W. Nahm, Y.K. Park, Property and performance of red mud-based catalysts for the complete oxidation of volatile organic compounds, J. Hazard. Mater. 300 (2015) 104–113.
[13] P. Topka, L. Kaluza, J. Gaalova, Total oxidation of ethanol and toluene over ceria-zirconia supported platinum catalysts, Chem. Pap. 70 (2016) 898–906.
[14] A.L. Marsh, D.J. Burnett, D.A. Fischer, J.L. Gland, In-situ Soft x-ray studies of toluene catalytic oxidation on the Pt(111) surface, J. Phys. Chem. B 108 (2004) 605–611.
[15] C.Y. Chen, F. Chen, L. Zhang, S.X. Pan, C.Q. Bian, X.M. Zheng, X.J. Meng, F.S. Xiao, Importance of platinum particle size for complete oxidation of toluene over Pt/ZSM-5 catalysts, Chem. Commun. 51 (2015) 5936–5938.
[16] Y.T. Lai, T.C. Chen, Y.K. Lan, B.S. Chen, J.H. You, C.M. Yang, N.C. Lai, J.H. Wu, C.S. Chen, Pt/SBA-15 as a highly efficient catalyst for catalytic toluene oxidation, ACS Catal. 4 (2014) 3824–3836.
[17] N. Burgos, M. Paulis, M.M. Antxustegi, M. Montes, Deep oxidation of VOC mixtures with platinum supported on Al_2O_3/Al monoliths, Appl. Catal. B: Environ. 38 (2002) 251–258.
[18] N. Radic, B. Grbic, A. Terlecki-Baricevic, Kinetics of deep oxidation of n-hexane and toluene over Pt/Al_2O_3 catalysts, Appl. Catal. B: Environ. 50 (2004) 153–159.
[19] Z. Abbasi, M. Haghighi, E. Fatehifar, S. Saedy, Synthesis and physicochemical characterizations of nanostructured Pt/Al_2O_3-CeO_2 catalysts for total oxidation of VOCs, J. Hazard. Mater. 186 (2011) 1445–1454.
[20] B. Zheng, G. Liu, L.L. Geng, J.Y. Cui, S.J. Wu, P. Wu, M.J. Jia, W.F. Yan, W.X. Zhang, Role of the FeO_x support in constructing high-performance Pt/FeO_x catalysts for low-temperature CO oxidation, Catal. Sci. Technol. 6 (2016) 1546–1554.
[21] B. Zheng, S. Wu, X. Yang, M. Jia, W. Zhang, G. Liu, Room temperature CO oxidation over Pt/$MgFe_2O_4$: a stable inverse spinel oxide support for preparing highly efficient Pt catalyst, ACS Appl. Mater. Interfaces 8 (2016) 26683–26689.
[22] J.H. Kwak, J. Hu, D. Mei, C.W. Yi, D.H. Kim, C.H. Peden, L.F. Allard, J. Szanyi, Coordinatively unsaturated Al^{3+} centers as binding sites for active catalyst phases of platinum on γ-Al_2O_3, Science 325 (2009) 1670–1673.
[23] J.C. Serrano-Ruiz, G.W. Huber, M.A. Sanchez-Castillo, J.A. Dumesic, F. Rodriguez-Reinoso, A. Sepulveda-Escribano, Effect of Sn addition to Pt/CeO_2-Al_2O_3 and Pt/Al_2O_3 catalysts: an XPS, ^{119}Sn Mössbauer and microcalorimetry study, J. Catal. 241 (2006) 378–388.
[24] L.D. Deng, H. Miura, T. Shishido, Z. Wang, S. Hosokawa, K. Teramura, T. Tanaka, Elucidating strong metal-support interactions in Pt-Sn/SiO_2 catalyst and its consequences for dehydrogenation of lower alkanes, J. Catal. 365 (2018) 277–291.
[25] H. Tang, Y. Su, Y. Guo, L. Zhang, T. Li, K. Zang, F. Liu, L. Li, J. Luo, B. Qiao, J. Wang, Oxidative strong metal-support interactions (OMSI) of supported platinum-group metal catalysts, Chem. Sci. 9 (2018) 6679–6684.
[26] H.B. Huang, D.Y.C. Leung, D.Q. Ye, Effect of reduction treatment on structural properties of TiO_2 supported Pt nanoparticles and their catalytic activity for formaldehyde oxidation, J. Mater. Chem. 21 (2011) 9647–9652.
[27] Y.X. Liu, H.X. Dai, J.G. Deng, X.W. Li, Y. Wang, H. Arandiyan, S.H. Xie, H.G. Yang, G.S. Guo, Au/3DOM $La_{0.6}Sr_{0.4}MnO_3$: highly active nanocatalysts for the oxidation of carbon monoxide and toluene, J. Catal. 305 (2013) 146–153.
[28] Q.J. Meng, J.J. Liu, X.L. Weng, P.F. Sun, J.A. Darr, Z.B. Wu, *In situ* valence modification of Pd/NiO nano-catalysts in supercritical water towards toluene oxidation, Catal. Sci. Technol. 8 (2018) 1858–1866.
[29] X. Chen, Z.L. Zhao, Y. Zhou, Q.L. Zhu, Z.Y. Pan, H.F. Lu, A facile route for spraying preparation of Pt/TiO_2 monolithic catalysts toward VOCs combustion, Appl. Catal. A Gen. 566 (2018) 190–199.
[30] C. He, F.W. Zhang, L. Yue, X.S. Shang, J.S. Chen, Z.P. Hao, Nanometric palladium confined in mesoporous silica as efficient catalysts for toluene oxidation at low temperature, Appl. Catal. B: Environ. 111 (2012) 46–57.
[31] S. Zhao, K. Li, S. Jiang, J. Li, Pd–Co based spinel oxides derived from pd nanoparticles immobilized on layered double hydroxides for toluene combustion, Appl. Catal. B: Environ. 181 (2016) 236–248.
[32] C. He, Q. Shen, M.X. Liu, Toluene destruction over nanometric palladium supported ZSM-5 catalysts: influences of support acidity and operation condition, J. Porous Mater. 21 (2014) 551–563.
[33] S.H. Xie, H.X. Dai, J.G. Deng, H.G. Yang, W. Han, H. Arandiyan, G.S. Guo, Preparation and high catalytic performance of Au/3DOM Mn_2O_3 for the oxidation of carbon monoxide and toluene, J. Hazard. Mater. 279 (2014) 392–401.
[34] J.L. Song, G.Y. Yu, X. Li, X.W. Yang, W.X. Zhang, W.F. Yan, G. Liu, Oxidative coupling of alcohols and amines to an imine over Mg-Al acid-base bifunctional oxide catalysts, Chin. J. Catal. 39 (2018) 309–318.
[35] X. Carrier, E. Marceau, J.F. Lambert, M. Che, Transformations of γ-alumina in aqueous suspensions: 1. Alumina chemical weathering studied as a function of pH, J. Colloid Interface Sci. 308 (2007) 429–437.
[36] M. Moses-DeBusk, M. Yoon, L.F. Allard, D.R. Mullins, Z. Wu, X. Yang, G. Veith, G.M. Stocks, C.K. Narula, CO oxidation on supported single Pt atoms: experimental and ab initio density functional studies of CO interaction with Pt atom on θ-Al_2O_3(010) surface, J. Am. Chem. Soc. 135 (2013) 12634–12645.
[37] Z. Zhang, Y. Zhu, H. Asakura, B. Zhang, J. Zhang, M. Zhou, Y. Han, T. Tanaka, A. Wang, T. Zhang, N. Yan, Thermally stable single atom Pt/m-Al_2O_3 for selective hydrogenation and CO oxidation, Nat. Commun. 8 (2017) 16100.
[38] P. Jing, T. Gan, H. Qi, B. Zheng, X. Chu, G. Yu, W. Yan, Y. Zou, W. Zhang, G. Liu, Synergism of Pt nanoparticles and iron oxide support for chemoselective hydrogenation of nitroarenes under mild conditions, Chin. J. Catal. 40 (2019) 214–222.
[39] K. Ding, A. Gulec, A.M. Johnson, N.M. Schweitzer, G.D. Stucky, L.D. Marks, P.C. Stair, Identification of active sites in CO oxidation and water-gas shift over supported Pt catalysts, Science 350 (2015) 189.
[40] M. Nagao, Y. Suda, Adsorption of benzene, toluene, and chlorobenzene on titanium dioxide, Langmuir 5 (1989) 42–47.
[41] A.J. Maira, J.M. Coronado, V. Augugliaro, K.L. Yeung, J.C. Conesa, J. Soria, Fourier transform infrared study of the performance of nanostructured TiO_2 particles for the photocatalytic oxidation of gaseous toluene, J. Catal. 202 (2001) 413–420.
[42] S. Besselmann, E. Loffler, M. Muhler, On the role of monomeric vanadyl species in toluene adsorption and oxidation on V_2O_5/TiO_2 catalysts: a Raman and in situ DRIFTS study, J. Mol. Catal. A: Chem. 162 (2000) 401–411.
[43] H. Sun, Z. Liu, S. Chen, X. Quan, The role of lattice oxygen on the activity and selectivity of the OMS-2 catalyst for the total oxidation of toluene, Chem. Eng. J. 270 (2015) 58–65.
[44] S. Hu, W. Xiao, W. Yang, J. Yang, Y. Fang, J. Xiong, Z. Luo, H. Deng, Y. Guo, L. Zhang, J. Ding, Molecular O_2 activation over Cu(I)-mediated C≡N bond for low-temperature CO oxidation, ACS Appl. Mater. Interfaces 10 (2018) 17167–17174.
[45] A. Gonchar, T. Risse, H.J. Freund, L. Giordano, C. Di Valentin, G. Pacchioni, Activation of oxygen on MgO: radical ion formation on thin, metal-supported MgO (001) films, Angew. Chem. Int. Ed. 50 (2011) 2635–2638.
[46] J.R. Katzer, G.C.A. Schuit, J.H.C. Van Hooff, Paramagnetic platinum and oxygen species on supported platinum, J. Catal. 59 (1979) 278–292.
[47] Y. Akdogan, C. Vogt, M. Bauer, H. Bertagnolli, L. Giurgiu, E. Roduner, Platinum species in the pores of NaX, NaY and NaA zeolites studied using EPR, XAS and FTIR spectroscopies, Phys. Chem. Chem. Phys. 10 (2008) 2952–2963.
[48] Y. Kratish, A. Kostenko, A. Kaushansky, B. Tumanskii, D. Bravo-Zhivotovskii, Y. Apeloig, Generation and characterization of the first persistent platinum(I)-Centered radical, Angew. Chem. Int. Ed. 57 (2018) 8275–8279.